Core–Shell Supramolecular Gelatin Nanoparticles for Adaptive and "On-Demand" Antibiotic Delivery

Li-Li Li,[†,⊥] Jun-Hua Xu,[†,‡,⊥] Guo-Bin Qi,[†,§] Xingzhong Zhao,[‡] Faquan Yu,[§] and Hao Wang[†,*]

[†]CAS Key Laboratory for Biological Effects of Nanomaterials and Nanosafety, National Center for Nanoscience and Technology (NCNST), No. 11 Beiyitiao, Zhongguancun, Beijing, China, [‡]Department of Physics, School of Physics, Wuhan University, Luo-jia-shan, Wuchang, Wuhan, 430072, China, and [§]Key Laboratory for Green Chemical Process of Ministry of Education, School of Chemical Engineering and Pharmacy, Wuhan Institute of Technology, No. 693 Xiongchu Avenue, Hongshan, Wuhan, 430073, China. [⊥]L.-L. Li and J.-H. Xu contributed equally to this work.

ABSTRACT The treatment of bacterial infection is one of the most challenging tasks in the biomedical field. Antibiotics were developed over 70 years and are regarded as the most efficient type of drug to treat bacterial infection. However, there is a concern that the overuse of antibiotics can lead to a growing number of multidrug-resistant bacteria. The development of antibiotic delivery systems to improve the biodistribution and bioavailability of antibiotics is a practical strategy for reducing the generation of antibiotic resistance and increasing the lifespan of newly developed antibiotics. Here we present an antibiotic delivery system (Van⊂SGNPs@RBC) based on core–shell supramolecular gelatin nanoparticles (SGNPs) for adaptive and "on-demand" antibiotic delivery. The core composed of cross-linked SGNPs allows for bacterial infection–microenvironment responsive release of antibiotics. The shell coated with uniform red blood cell membranes executes the function of disguise for reducing the clearance by the immune system during the antibiotic delivery, as well as absorbs the bacterial exotoxin to relieve symptoms caused by bacterial infection. This approach demonstrates an innovative and biomimetic antibiotic delivery system for the treatment of bacterial infection with a minimum dose of antibiotics.

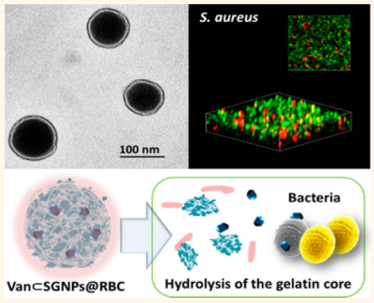

KEYWORDS: supramolecular · gelatin nanoparticles · vancomycin · antibacterial · drug delivery

The treatment of bacterial infection related diseases has attracted wide attention in the past few decades.[1] Since the development of antibiotics in the 1940s, millions of patients' lives have been saved.[2] However, the abuse of antibiotics leads to the appearance of antibiotic-resistant species such as superbugs and therefore encourages us to create an "on-demand" use of antibiotics.[3−6] Currently, numerous antibiotic replacements, *e.g.*, inorganic nanoparticles,[7−14] photothermal/photodynamic agents,[15,16] antimicrobial peptides,[17−19] and cationic polymers,[20−25] have been reported to decrease the possibility of antibiotic resistance. Aimed toward blind therapy in clinical practice, an innovative antibiotic nanodelivery system[26−29] is now a powerful tool to circumvent antibiotic resistance.[30] Among these nanocarriers, two categorized design strategies prove to be promising in the treatment of bacterial infections and related diseases: (i) the transportation of antibiotics to immune cells *via* a phagocytic pathway and subsequent release of cargoes against intracellular infections[26,31,32] and (ii) the delivery of antibiotics to the infection area and their site-specific release by activation of the infection–microenvironment responsive mechanism.[33,34] Nevertheless, the effective release of antibiotics in an infection microenvironment tends to always encounter the obstacle of rapid immune clearance,[35] which dramatically decreases delivery efficiency and drug bioavailability.[36] Therefore, an emerging challenge in the field of material science and nanomedicine[37,38] lies in the encapsulation of antibiotics in nanoparticles, keeping them hidden under the radar of the innate immune system, and the eventual release of payloads in the regions of interest.

The supramolecular approach enables flexible and modular preparation of nanocarriers with desirable features.[39−45] By tailoring the function of individual building blocks and noncovalent interactions with each other, the structure and function of the

* Address correspondence to wanghao@nanoctr.cn.

Received for review February 21, 2014 and accepted April 9, 2014.

Published online April 09, 2014
10.1021/nn501040h

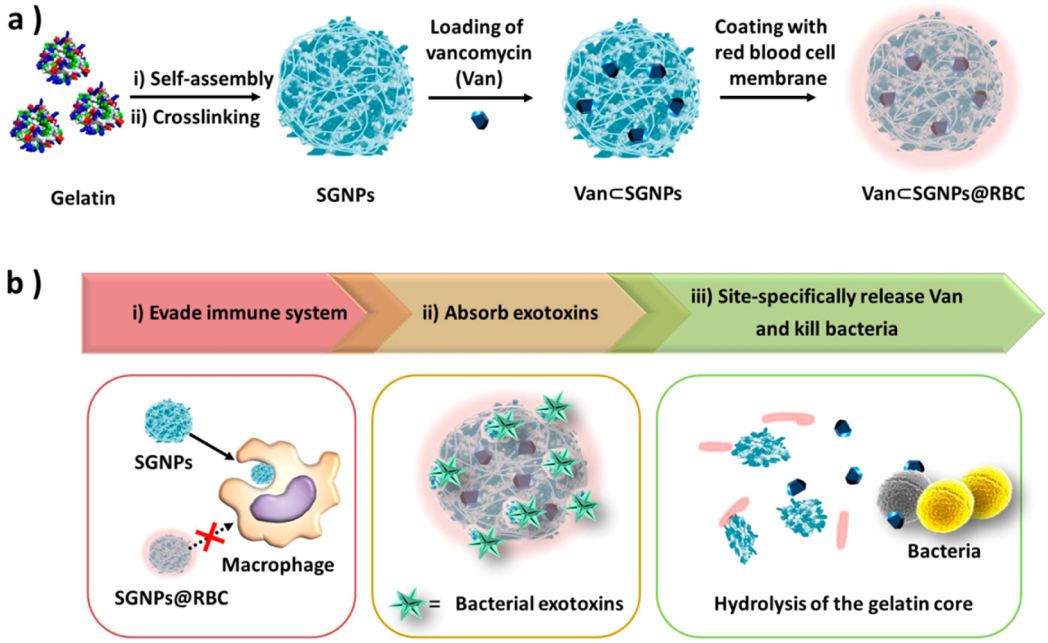

Scheme 1. (a) Preparation of vancomycin encapsulated supramolecular gelatin nanoparticles with RBC membrane coating layer (Van⊂SGNPs@RBC). (b) Schematic representation of adaptive and multifunctional Van⊂SGNPs@RBC in the treatment of a bacterial infection.

resulting self-assembled carriers can be controlled on-demand.[46−50] Previously, we improved the formulation and manufacturing method[51,52] for robust and reliable preparation of size-controllable supramolecular gelatin nanoparticles that can disassemble in the presence of matrix metalloproteinases (MMPs).[53] It is well known that a broad spectrum of bacteria secrete gelatinases,[54] including MMP-2 and MMP-9, which also effectively hydrolyze gelatin nanoparticles into small biomolecules.[55]

Herein, we report an adaptive and "on-demand" antibiotic delivery system based on supramolecular gelatin nanoparticles (SGNPs) by activation of their release mechanism in the presence of gelatinase at the bacterial infection site. The surfaces of SGNPs were decorated with red blood cell (RBC) membranes (SGNPs@RBC), and vancomycin (Van), as a model antibiotic, was further encapsulated in SGNPs@RBC as the interior (Van⊂SGNPs@RBC, Scheme 1). The coating of RBC membranes imparts a biomimetic characteristic to Van⊂SGNPs@RBC and significantly improves the immune-evading capability of the resulting nanocarriers, which are capable of effectively accumulating at the infection site *via* enhanced permeability and retention effects.[56] After arriving at the infection microenvironment, the RBC membranes on the Van⊂SGNPs@RBC act as detoxifiers to enable further absorption of the exotoxins that are produced by bacteria and relieve the symptoms caused by them. Meanwhile, the gelatin core is degraded by the gelatinase that is overexpressed in the infection microenvironment, and the encapsulated Van is subsequently released and kills pathogenic bacteria locally. This approach demonstrates an innovative and biomimetic antibiotic delivery system for the treatment of bacterial infection with a minimum dose of antibiotics. The proof-of-concept study of this work may prove to be helpful for reducing the generation of antibiotic resistance and increasing the lifespan of newly developed antibiotics.

RESULTS AND DISCUSSION

Preparation and Characterization of Van⊂SGNPs@RBC. SGNPs were prepared by using the desolvation method[51,52] according to our previously reported procedure.[53,57] The fresh isolated membranes from RBCs were mixed with SGNPs, and the resulting mixture was extruded on an Avanti mini-extruder to ensure uniform coating (for details see Methods). To visualize the coating of the RBC membrane onto SGNPs, transmission electron microscopy (TEM) was carried out to observe the morphology and core−shell structures of SGNPs@RBC (Figure 1a). Compared to the SGNPs, with a size of 84.5 ± 4.8 nm, the SGNPs@RBC unambiguously showed a spherical core−shell structure with slightly increased size up to 97.3 ± 3.4 nm. The thickness of the coating membrane was approximately 7 nm, which corresponds to the RBC membrane of 5−10 nm[58] (Figure S1). After absorption of streptolysin O (SLO), one of the pore-forming exotoxins secreted by *Streptococcus pyogenes*,[59] the RBC membrane of the SGNPs@RBC became porous, suggesting that the SLO molecules were inserted into the RBC membrane of SGNPs@RBC and then formed a porous SLO assembly[59] (Figure S2). Furthermore, dynamic light scattering (DLS, Figure 1b) results indicated that the hydrodynamic diameters of SGNPs increased from

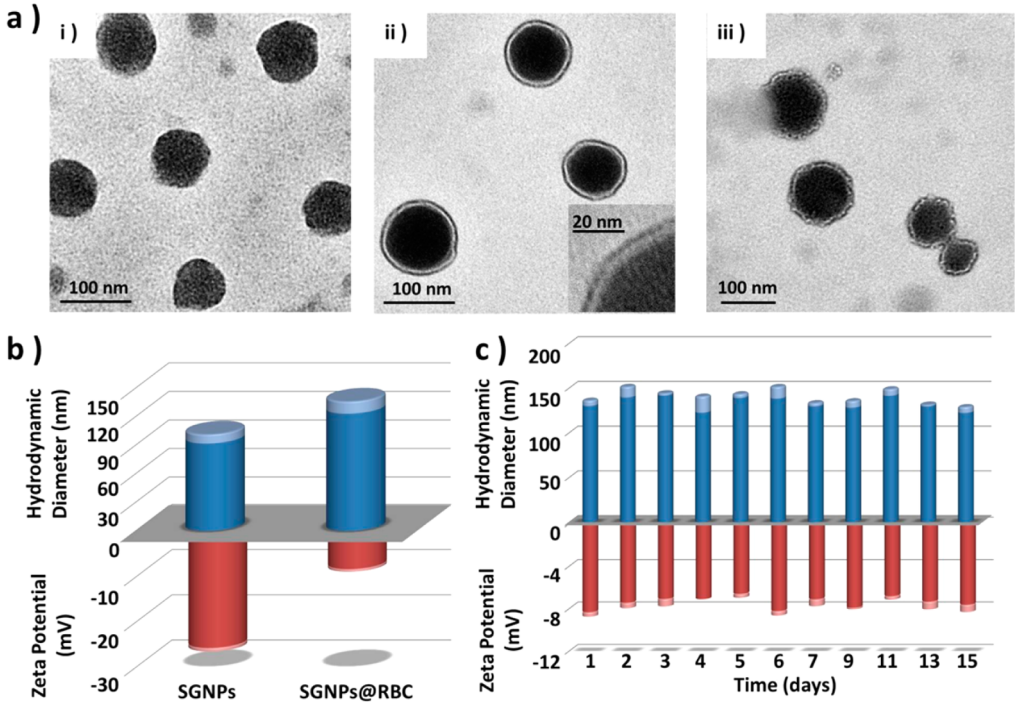

Figure 1. Characterizations of SGNPs@RBC. (a) TEM images of (i) SGNPs, (ii) SGNPs@RBCs, and (iii) toxin-absorbing SGNPs@RBC. The TEM images show the distinct core−shell structure of the SGNPs@RBC and the porous surface of SGNPs@RBC after being treated with streptolysin O (SLO, exotoxin secreted from *S. pyogenes*). (b) Hydrodynamic diameters (blue) and zeta potentials (red) of SGNPs and SGNPs@RBC. (c) The stability of SGNPs@RBC in cell culture medium (DMEM) containing 10% serum was tested by monitoring the size and zeta potential changes over a span of 15 days. All values are expressed as mean ± SD (n = 6), and the experiment was repeated independently at least twice.

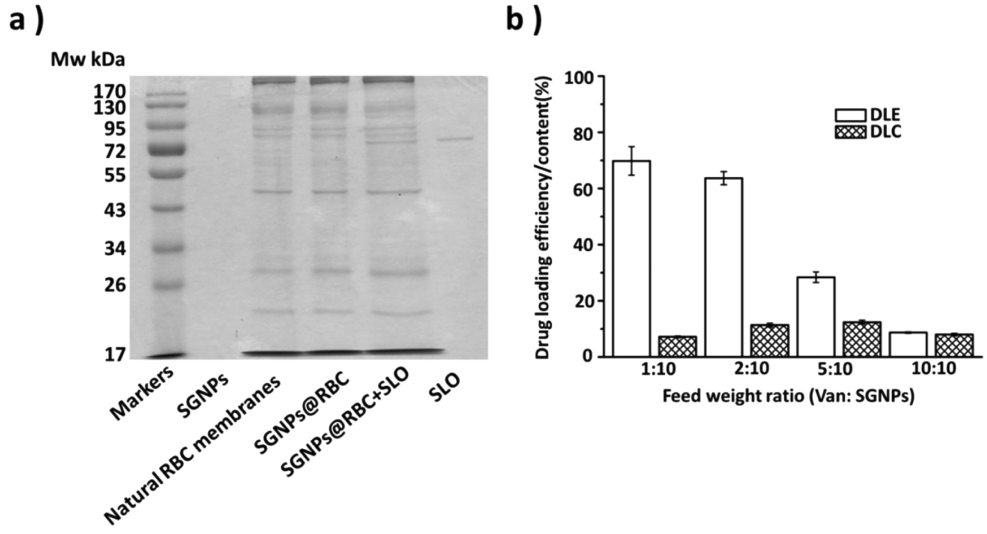

Figure 2. Toxin absorption and Van loading of Van⊂SGNPs@RBC. (a) SDS-PAGE of SGNPs@RBC along with SGNPs, natural RBC membranes, SLO, and SLO-absorbing SGNPs@RBC. (b) Drug loading content (DLC) and drug loading efficiency (DLE) of Van⊂SGNPs@RBC with a weight ratio of Van to SGNPs of 1:10, 2:10, 5:10, and 10:10, respectively.

91.9 ± 9.5 nm to 123.3 ± 12.7 nm upon coating with the RBC membrane vesicles. Accordingly, the zeta potentials also changed from −26.16 ± 0.8 mV to −8.7 ± 0.6 mV. Moreover, the stability of the SGNPs@RBC in normal cell culture medium was monitored by DLS and zeta potential techniques, and the results showed that the SGNPs@RBC were stable in the medium up to 15 days (Figure 1c). Additionally, sodium dodecyl sulfate polyacrylaminde gel electrophoresis (SDS-PAGE) experiments of SGNPs@RBC along with SGNPs, natural RBC membranes, SLO, and SLO-absorbing SGNPs@RBC were performed in parallel (Figure 2a). Compared with natural RBC membranes, the majority of endogeous membrane proteins were not lost during the sample preparation. In addition, the remarkable toxin absorption was observed after treatment of

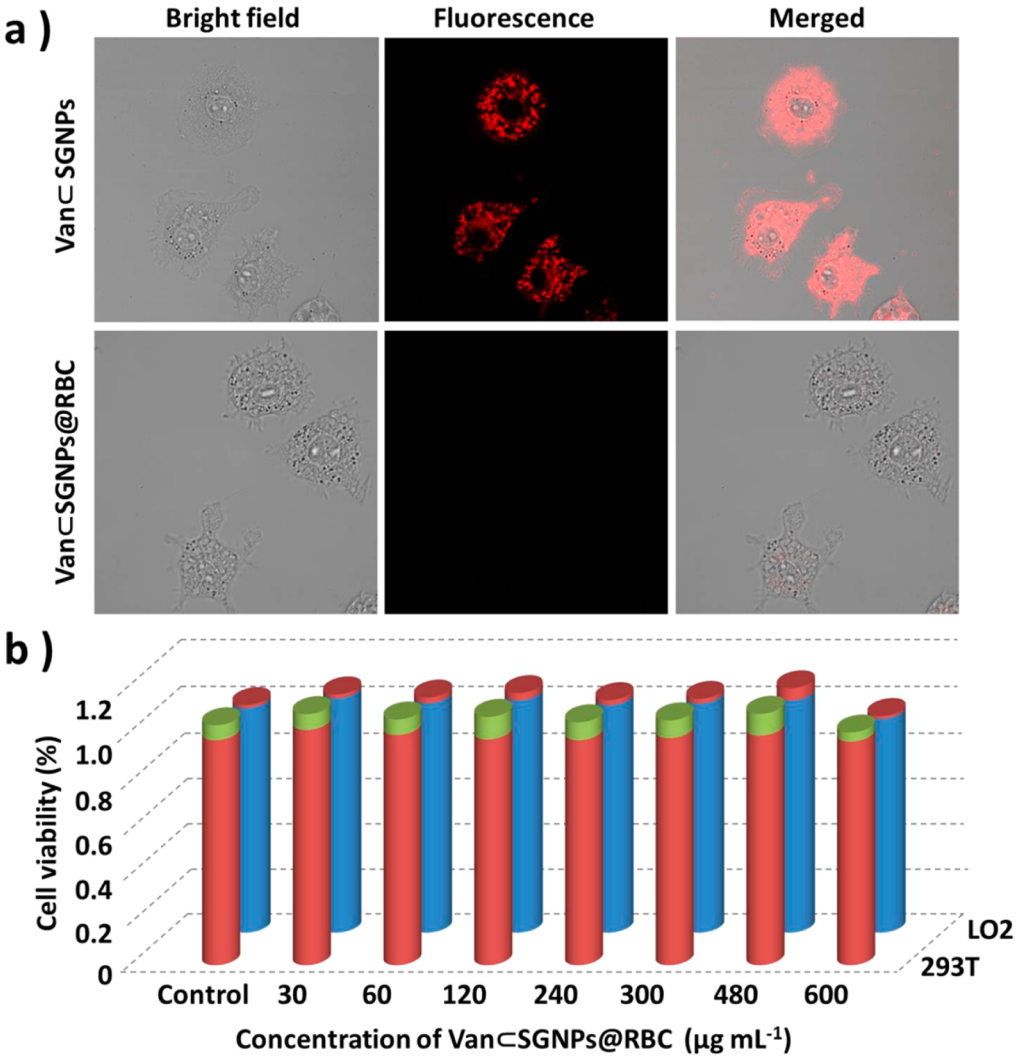

Figure 3. Immune-evading capability and biocompatibility of Van⊂SGNPs@RBC. (a) Fluorescence images of RAW 264.7 (macrophage cell line) cells treated by Van⊂SGNPs@RBC and Van⊂SGNPs, respectively. The Cy5-labeled nanoparticles (50 μg mL^{-1}) were incubated with cells at 37 °C for 30 min. The cells were washed with PBS three times prior to image acquisition. (b) Cell availability of human embryonic kidney (293T) and human hepatocyte (LO2) cell lines upon treatment with a series of concentrations of Van⊂SGNPs@RBC (0−600 μg mL^{-1}).

SGNPs@RBC with SLO, suggesting high toxin absorption and clearance capability of the nanoparticles. To efficiently encapsulate Van into SGNPs to form Van⊂SGNPs@RBC, the lyopholized SGNP powder was swollen in a Van-containing PBS solution (c = 10 mg mL^{-1}) for 24 h; then the free Van was removed by dialysis overnight and coated with RBC membranes. The drug loading efficiency (DLE) and drug loading content (DLC) were determined by HPLC (Supporting Information, Figure S3). The optimal formulation of Van⊂SGNPs@RBC with a DLE of 63.7% and DLC of 11.4% was obtained by feeding Van:SGNPs = 2:10 (w/w) (Figure 2b) and used for the following experiments.

Immune-Evading Capability and Biocompatibility of Van⊂SGNPs@RBC. The immune-evading capability of Van⊂SGNPs@RBC was examined by antiphagocytosis against macrophage cells. For the purpose of tracking and comparison, the Van⊂SGNPs@RBC and Van⊂SGNPs were labeled with Cy5 (see Methods). The Cy5-labeled Van⊂SGNPs@RBC and Van⊂SGNPs (50 μg mL^{-1}) were incubated with RAW 264.7 macrophage cells for 30 min at 37 °C (5% CO_2). A confocal laser scanning microscope was utilized to visualize the uptake of the nanoparticles by RAW 264.7 cells (Figure 3a). The Van⊂SGNPs@RBC were barely internalized by macrophage cells compared to Van⊂SGNPs, indicating that the RBC membrane coating layer can successfully avoid recognition by immune cells. Moreover, the negligible cytotoxicity of Van⊂SGNPs@RBC toward human embryonic kidney (293T) and human hepatocyte (LO2) cell lines implied high biocompatibility of our drug delivery system (Figure 3b).

Release Profiles of Van from Van⊂SGNPs@RBC. To demonstrate that the release of Van from Van⊂SGNPs@RBC was triggered by gelatinase, the release profiles of Van⊂SGNPs@RBC were carried out by using HPLC (Figure 4a). The Van⊂SGNPs@RBC (3 mg mL^{-1})

were incubated in the presence of gelatinase with variable concentrations from 0 to 1.5 mg mL^{-1} in a Tris buffer (20 mM Tris·HCl, 50 mM NaCl, 5 mM $CaCl_2$, 0.05% Brij-35, pH 7.4) for 50 h (for more details see Supporting Information, Figure S4). As shown in Figure 3a, maximal cumulative Van release (*ca.* 79.6%) was reached within 4 h under gelatinase with a concentration of 0.3 mg mL^{-1}. The release process slowed down and the release peak was achieved after 48 h in the presence of gelatinase with a concentration of 7.5 μg mL^{-1}. In sharp contrast, only 17.6% Van was released after 50 h without gelatinase. In addition, the Van⊂SGNPs@RBC show remarkably decreased drug release efficiency compared to Van⊂SGNPs. The release of Van from Van⊂SGNPs reached 60% in the presence of gelatinase (0.5 μg mL^{-1}, Figure S5) within 1 h, while only less than 25% of Van was released from Van⊂SGNPs@RBC under the same condition. Meanwhile, the Van release from Van⊂SGNPs@RBC can also be promoted with the pore-forming toxin of SLO (Supporting Information, Figure S6). All these results implied that the Van⊂SGNPs@RBC were a gelatinase concentration/time-dependent delivery system. To evaluate the Van release performance of Van⊂SGNPs@RBC toward different species of bacteria, the cumulative release curves of Van⊂SGNPs@RBC against a broad spectrum of bacteria, *i.e.*, *S. aureus*, *E. coli*, *S. epidermidis*, *P. vulgaris*, *S. marcescens*, and *P. aeruginosa*, were determined (Figure 4b). Upon co-incubation with gelatinase-positive bacterial species (5×10^8 cfu) such as *S. aureus*, *P. vulgaris*, *S. marcescens*, and *P. aeruginosa*, 62.4−91.7% Van was released from Van⊂SGNPs@RBC (3 mg mL^{-1}), while a cumulative release of 20% was reached in gelatinase-negative bacteria (*E. coli* and *S. epidermidis*) or the pure bacterial culture medium (tryptic soy broth). The degradation property of Van⊂SGNPs@RBC in an infection microenvironment would show the site-specific and on-demand release of antibiotics with a minimal dose.

Toxin-Removing Capability and Specific Responsiveness of Van⊂SGNPs@RBC. Finally, we examined the toxin-removing capability of SGNPs@RBC through antihemolytic experiments. The antihemolytic activity of SGNPs@RBC was determined by measuring the hemoglobin released from the damaged RBCs[60] (Supporting Information, Figure S7). As can be seen from Figure 5a, the SGNPs@RBC themselves exhibited relatively lower hemolysis (<4%) compared to that of PBS and SGNP control groups. However, a remarkable SLO clearance ability and antihemolytic activity of SGNPs@RBC (2.5 mg mL^{-1}) were observed in the presence of SLO (100 U per mL full blood) compared to that of PBS and SGNP control groups. Furthermore, the detoxification efficacy of SGNPs@RBC to various bacterial species was carried out by measuring the hemolytic effect (Figure 5b). As shown in Table 1 and Table S1, the hemolysis of RBCs in the presence of all six bacteria

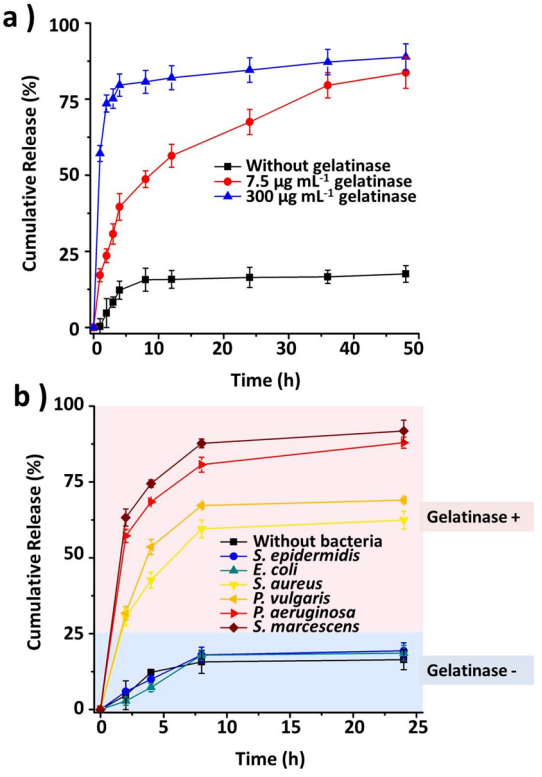

Figure 4. Release profiles of Van⊂SGNPs@RBC in the presence of gelatinase or different bacteria. (a) Representative time-dependent Van release curves of Van⊂SGNPs@RBC under different concentrations of gelatinase (0, 7.5, and 300 μg mL^{-1}) up to 50 h. (b) The cumulative release of Van of Van⊂SGNPs@RBC (3 mg mL^{-1}) exposed to various bacterial strains (5×10^8 cfu) at 37 °C for 24 h. All values are expressed as mean ± SD (n = 3), and the experiments were repeated independently at least twice.

significantly decreased upon treatment by SGNPs@RBC. For instance, the hemolysis caused by *P. vulgaris* (from 64.7% to 1.9%), *S. marcescens* (from 100.0% to 36.4%), and *P. aeruginosa* (from 35.0% to 2.4%) was dramatically improved upon treatments by SGNPs@RBC, which was ascribed to the detoxification property of the RBC membrane. Besides the improved hemolysis, the specificity of antibacterial efficacy of Van⊂SGNPs@RBC was tested. *S. aureus* and *S. epidermidis* as gelatinase-positive and gelatinase-negative bacteria were chosen as model strains. Van⊂SGNPs@RBC (5 mg mL^{-1}) were added into the bacteria medium for 4 h, and the bacteria cells subsequently were stained with live/dead cell staining kits. Both 2D and 3D confocal microscope images (Figure 5c) were obtained, and the results revealed that Van⊂SGNPs@RBC showed higher antibacterial efficacy toward *S. aureus* than toward *S. epidermidis*, which was attributed to the promoted degradation of the gelation core of Van⊂SGNPs@RBC and release of Van to kill the gelatinase-positive *S. aureus*. Quantitatively, we measured the minimum inhibitory concentration (MIC) of Van⊂SGNPs@RBC and Van⊂SGNPs toward a series of Gram-positive and Gram-negative bacteria (Table 1 and Table S1). We did not find the

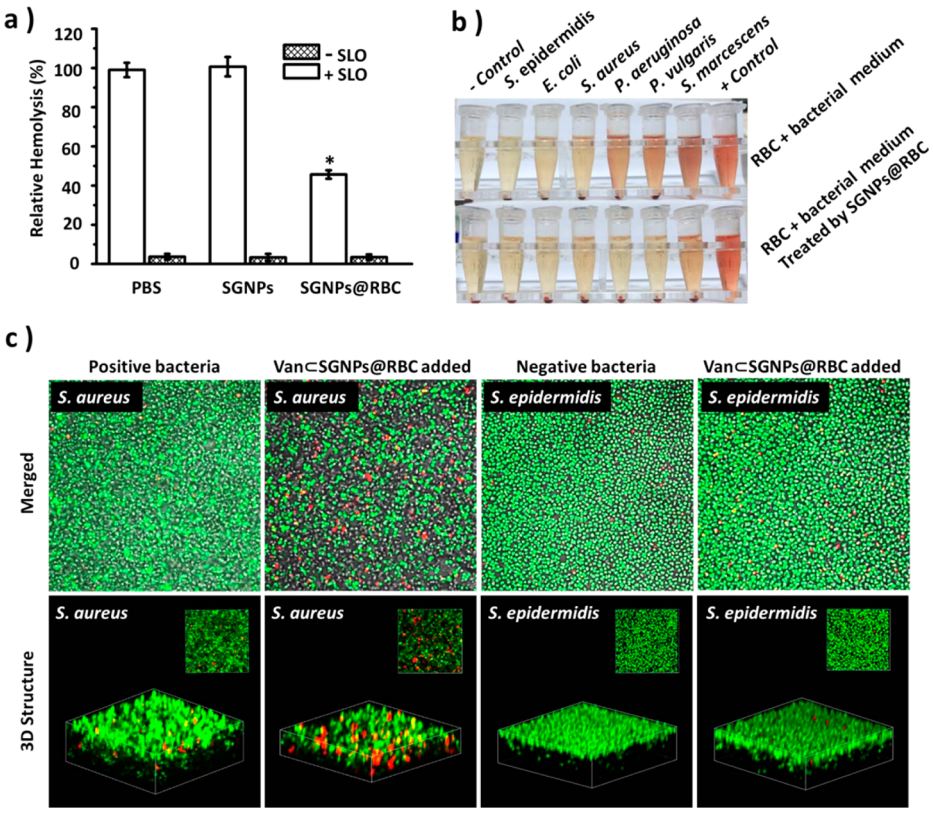

Figure 5. Toxin-removing capability and specific responsiveness of Van⊂SGNPs@RBC. (a) Hemolysis quantification of RBCs incubated with or without SLO (100 U per mL full blood) in PBS, SGNPs, and SGNPs@RBC (2.5 mg mL^{-1}). (b) Photographs of the antihemolysis of SGNPs@RBC to different species of bacteria with a negative control of tryptic soy broth (TSB) solution and a positive control of 1% Triton X-100 TSB solution. (c) 2D and 3D structure of confocal microscope images of inhibition and killing of bacteria by Van⊂SGNPs@RBC exposed to gelatinase-positive bacteria (*S. aureus*) and gelatinase-negative bacteria (*S. epidemidis*).

TABLE 1. Antihemolysis and Minimum Inhibitory Concentration (MIC) of Van⊂SGNPs@RBC for Various Bacterial Species

species		gelatinase[a]	hemolysis[b] (%)	MIC[c] (μg mL^{-1})
Gram-positive	*S. epidermidis*	−	0.16 ± 0.01 (0.18 ± 0.01)	12 ± 1.4 (1.5 ± 0.5)
	S. aureus	+	10.0 ± 0.51 (16.5 ± 0.18)	3 ± 0.8 (1.5 ± 0.5)
Gram-negative	*E. coli*	−	1.6 ± 0.27 (2.3 ± 0.29)	>500 (250 ± 5.3)
	P. vulgaris	+	1.9 ± 0 0.67 (67.4 ± 0.64)	>500 (500 ± 10.7)
	S. marcescens	+	36.4 ± 1.38 (100.0 ± 2.61)	− (>500)
	P. aeruginosa	+	2.4 ± 0.31 (35.0 ± 1.28)	− (>500)

[a] The classification of gelatinase-positive and gelatinase-negative bacteria refers to ref 24. [b] The hemolysis percentage was calculated from the following equation: Hemolysis % = $(A_S - A_-)/(A_+ - A_-) \times 100\%$, where A_S is the absorbance of bacterial sample (RBCs with supernatant solution of bacteria) at 405 nm, A_- is the absorbance of the negative control (RBCs in TSB solution), and A_+ is the absorbance of the positive control (RBCs in TSB solution with 0.1% Triton X-100) at 405 nm, respectively. The bacterial samples (1 mL, OD_{600} = 0.5 bacterial TSB solution) were mixed with SGNPs@RBC (400 μL, 150 μg mL^{-1}) at 37 °C for 2 h and then mixed with RBCs (12 μL of full blood) for another 2 h. [c] The concentration of Van⊂SGNPs@RBC was calculated based on the content of encapsulated Van.

obvious inhibition effect of Van⊂SGNPs@RBC for Gram-negative bacteria even with a concentration of up to 500 μg mL^{-1}, owing to the poor recognition by Van of Gram-negative bacteria. Among the Gram-positive bacteria, a remarkable MIC value (12 ± 1.4 μg mL^{-1}) was obtained upon treatment of *S. epidermidis* (a gelatinase-negative strain) with Van⊂SGNPs@RBC. Interestingly, an even smaller MIC value (3 ± 0.8 μg mL^{-1}) was observed for *S. aureus* (a gelatinase-positive strain). This low treatment dose was comparable with that of free Van (1.5 ± 0.5 μg mL^{-1}). All these results indicated that Van⊂SGNPs@RBC prefers to specifically kill Gram-positive and gelatinase-positive bacteria.

CONCLUSIONS

In summary, a new antibiotic delivery system (Van⊂SGNPs@RBC) has been developed for efficient and specific release of antibiotics in the infection site. Van⊂SGNPs@RBC enables on-demand delivery of antibiotics with biomimetic and detoxifying characteristics. By coating the RBC membranes, Van⊂SGNPs@RBC show

significant immune-evading and toxin-clearance capabilities. Meanwhile, the site-specific degradation of the nanoparticles endows this delivery system with a superb killing effect for Gram-positive and gelatinase-positive pathogenic bacteria with minimum systemic toxicity. We believe that the killing of bacteria with high efficacy and specificity can be achieved by alteration of different antibiotics and bioresponsive materials in the future.

MATERIALS AND METHODS

Materials. Bovine bone type-B gelatin, gelatinase, streptolysin O, vancomycin, glutaraldehyde, ethylenediaminetetraacetic acid (EDTA), uranium acetate, dithiothreitol, and bovine serum albumin (BSA) were purchased from Sigma-Aldrich Chemical Co. Dulbecco's modified Eagle's medium (DMEM), penicillin, streptomycin, ampicillin, fetal bovine serum (FBS), and trypsin were obtained from HyClone/Thermo Fisher (Beijing, China). RAW 264.7, 293T, and LO2 cell lines were purchased from Cell Culture Center of Institute of Basic Medical Sciences, Chinese Academy of Medical Sciences (Beijing, China). Cell counting kit (CCK-8) and tryptic soy broth (TSB) were obtained from Beyotime Institute of Biotechnology (Shanghai, China). Culture plates (96-well) were purchased from Corning Company. Sulfo-Cy5 NHS ester was obtained from Lumiprobe Corporation. The bacteria strains of *Staphylococcus aureus* (ATCC 6538), *Escherichia coli* (ATCC 8739), *Staphylococcus epidermidis* (ATCC 12228), *Proteus vulgaris* (ATCC 13315), *Serratia marcescens* (ATCC 14756), and *Pseudomonas aeruginosa* (ATCC 10145) were obtained from China General Microbiological Culture Collection Center. An Inertsil C_{18} HPLC column (ODS-3, 3 μm, 4.6 $\times$ 150 mm) for peptide analysis was purchased from Shimadzu Corporation. The HPLC grade solvents methanol and acetonitrile were purchased from Sigma-Aldrich and Fisher Scientific. Female BALB/c mice for collection of RBCs were purchased from Vital River Laboratory Animal Technology Co., Ltd. (Beijing, China). All the other solvents used in the research were purchased from Sinopharm Chemical Reagent Beijing Co., Ltd. or Beijing (China) Chemical Company.

Synthesis of Supramolecular Gelatin Nanoparticles. The supramolecular gelatin nanoparticles were prepared using a desolvation technique according to the literature.[52,53] An aqueous gelatin (type B) solution (0.5% w/v, 100 mL) was prepared. The pH was adjusted to 6 by the addition of NaOH (0.1 M). Then the solution was stirred at 50 °C and 100 rpm to obtain a clear solution, after which it was cooled and then filtered. To induce the desolvation process, acetone was added until a permanent faint turbidity was obtained. Finally, glutaraldehyde aqueous solution (25% v/v, 2 mL) was added to harden the particles. The preparation was then stirred for 2 h at 1000 rpm. The cross-linking was stopped by the addition of an aqueous sodium metabisulfite solution (1.2 g in 300 mL). The nanoparticle-formed solution was separated by centrifugation at 10 000 rpm for 10 min, washed three times with distilled water, then resuspended and dispersed in 100 mL of distilled water for use. The Cy5-labeled SGNPs were prepared by mixing Cy5-NHS with nanoparticles for 30 min and purified by centrifuging, separating the free molecules of Cy5-NHS.

Loading of Van into SGNPs. To efficiently encapsulate the Van into SGNPs to form Van⊂SGNPs, the lyophilized SGNP powder was first obtained. Then, the different weight of Van with a final concentration of 10 mg mL^{-1} was added into the lyophilized powder of SGNPs with a weight ratio of Van to SGNPs of 1:10, 2:10, 5:10, and 10:10, respectively. After swelling and loading of Van into SGNPs for 24 h at RT, the nanoparticles were purified by dialysis (Spectra/Por 4, MWCO 12 000 to 14 000) against DI water overnight to remove the unloaded free Van. To determine the drug loading efficiency and drug loading content of Van, the nanoparticles were centrifuged and the concentration of Van in the supernatant was measured by RP-HPLC (2535, Waters, with a C_{18} column and UV detector). The standard curve of Van was fitted with the peak area (0.025 M potassium dihydrogen phosphate buffer/methanol, 80/20 v/v, R_f = 9.2 min, 230 nm) and concentration of Van.

Preparation of RBC Membrane. The whole blood was collected from the orbit of female BALB/c mice with 1.5 mg of EDTA per mL of blood for anticoagulation. The blood was centrifuged at 3000 rpm for 5 min at 4 °C to remove the plasma and the buffy coat. The resulting RBCs were washed three times with ice cold 1$\times$ PBS. Then, 0.25$\times$ PBS was added for hemolysis *via* a hypotonic medium treatment in an ice-bath for 30 min. The released hemoglobin was removed by centrifugation with a speed of 14000 rpm for 5 min, and the pellet with a light pink color was collected and washed by 1$\times$ PBS twice. The RBC membrane was prepared by serially extruding through 200 nm polycarbonate porous membranes with an Avanti mini-extruder (Avanti Polar Lipids).

Preparation of RBC-Membrane-Coated Supramolecular Gelatin Nanoparticles. To coat the RBC membrane onto the SGNPs or Van⊂SGNPs, the SGNPs or Van⊂SGNPs (0.5 mg mL^{-1}, 500 μL) were mixed with 500 μL of RBC membrane prepared from whole blood. The mixture was extruded 11 times through a 200 nm polycarbonate porous membrane with an Avanti mini-extruder.[37] Finally, the newly prepared SGNPs@RBC or Van⊂SGNPs@RBC were left in PBS buffer overnight at 4 °C for further use.

Characterization of SGNPs@RBC. The hydrodynamic diameter and zeta potential were measured by DLS with a Zetasizer Nano instrument (Malvern Instruments, Malvern, UK). The morphology and sizes of SGNPs, SGNPs@RBC, and streptolysin O (SLO)-absorbing SGNPs@RBC were examined using a transmission electron microscope. The studies were carried out on a Tecnai G2 20 S-TWIN electron microscope operating at an accelerating voltage of 200 keV. The TEM samples were prepared by contacting the nanoparticle droplets with copper grids for 30 s, removing the excess droplets, and staining by uranyl acetate for 10 s before the TEM studies. Stability experiments of the SGNPs@RBC were carried out by measuring the mixture of SGNPs@RBC in DMEM medium with FBS for 2 weeks using DLS. The proteins reserved on the SGNPs@RBC as compared with the natural RBC membranes were observed by SDS-PAGE.

Hemolysis Study. The toxin-removing capability of SGNPs@RBC for exotoxins secreted from various types of bacteria was determined through antihemolytic experiments. The toxin-clearing ability of the SGNPs@RBC for streptolysin O (as model toxin) was examined by mixing 100 U of SLO (postactivated by incubation with 200 μM dithiothreitol in 500 μL of PBS containing 0.1% BSA) with SGNPs@RBC (2.5 mg) for 30 min, followed by adding 1 mL of full blood RBCs. The released hemoglobin from the broken RBCs in the supernatant was measured upon absorbance at 405 nm. The detoxification capability of various species of bacteria was carried out by measuring the hemolysis of RBCs due to bacteria with or without treatment by SGNPs@RBC. The detoxification of the bacterial medium by SGNPs@RBC was performed by incubating the supernatant of the bacteria solution (1 mL, OD_{600} = 0.5) with SGNPs@RBC (400 μL, 150 μg mL^{-1}) at 37 °C for 2 h. The hemolysis by the exotoxin of the bacteria was examined by incubating 12 μL of full blood RBCs with the supernatant of the bacteria medium or SGNPs@RBC-treated bacteria medium at 37 °C for 2 h. The released hemoglobin was quantified to determine the degree of RBC lysis.

Responsive Release of Van. The release profiles of Van from Van⊂SGNPs@RBC exposed to gelatinase or different species of bacteria were carried out by measuring the cumulative release over time. To demonstrate that the release of Van from Van⊂SGNPs@RBC was triggered by gelatinase, the release profiles of Van⊂SGNPs@RBC were determined by using HPLC. Van⊂SGNPs@RBC in Tris buffer (20 mM Tris·HCl, 50 mM NaCl, 5 mM $CaCl_2$, 0.05% Brij-35, pH 7.4) with gelatinase concentrations of 0−1.5 mg mL^{-1} were introduced to the tube at 30 °C for 48 h, and the released Van from Van⊂SGNPs@RBC at different time intervals was analyzed with HPLC. The bacterial responsive release of Van⊂SGNPs@RBC was obtained by adding

Van⊂SGNPs@RBC (3 μg mL^{-1}) into the culture medium of *S. aureus*, *E. coli*, *S. epidermidis*, *P. vulgaris*, *S. marcescens*, and *P. aeruginosa* with an optical density at 600 nm (OD_{600}) of 0.5 and incubating them at 37 °C for 24 h. At predetermined intervals, the samples were centrifuged and the released Van in the supernatants was analyzed by RP-HPLC.

Macrophage Uptake Study. The immune-evading capability of the Van⊂SGNPs@RBC was examined by antiphagocytosis against macrophage cells. The RAW 264.7 macrophage cells were cultured in DMEM medium with 10% FBS and seeded with a density of 10^5 cells per well in a 24-well plate. Final concentrations of Cy5-labeled Van⊂SGNPs@RBC and Van⊂SGNPs (50 μg mL^{-1}, respectively) were added into the macrophage cell culture medium. To examine the macrophage uptake of Van⊂SGNPs@RBC and Van⊂SGNPs, the nanoparticles were incubated with macrophage cells for 30 min and then washed with PBS. The quantification of the uptake by macrophage cells was imaged with a confocal laser scanning microscope with a ×100 oil-immersion objective lens using a 488 nm laser (Carl Zeiss AG, LSM780).

Minimum Inhibitory Concentration of Van⊂SGNPs@RBC. *S. aureus*, *E. coli*, *S. epidermidis*, *P. vulgaris*, *S. marcescens*, and *P. aeruginosa* were cultured in TSB media at 37 °C on a shaker bed at 200 rpm for 4−6 h. Then the concentration of bacteria was measured by UV−vis spectroscopy (Cary100Bio) corresponding to an optical density of 0.1 at 600 nm for 1×10^8 cfu mL^{-1}. The bacterial suspension (20 μL of 1×10^6 cfu mL^{-1}) and culture broth (160 μL) were seeded into each well of the Corning 96-well plate. Then PBS (20 μL, as the blank assay), Van, or Van⊂SGNPs@RBC were respectivly added into the plate and cultured with bacteria at 37 °C on a shaker bed at 200 rpm for 18 h. The data were determined by OD_{600} using a multifunctional microplate reader (Tecan Infinite M200). Cultures were prepared in triplicate, and all experiments were repeated twice or more.

Cytotoxicity Assay of Van⊂SGNPs@RBC. Human embryonic kidney 293T and human hepatocytes LO2 were cultured in DMEM (500 mL of DMEM mixed with 50 mL of fetal bovine serum, 50 000 units of penicillin, and 50 000 units of streptomycin). The third-generation 293T and LO2 cells (1×10^4 cells per well) were incubated with different concentrations of Van⊂SGNPs@RBC (30, 60, 120, 240, 300, 480, and 600 μg mL^{-1}) in DMEM medium (200 μL) for 24 h in a 96-well plate. After discarding the supernatant, CCK-8 DMEM solution (200 μL, 10%, volume ratio) was added, and the samples were incubated at 37 °C for 4 h. The absorbance at 450 nm with a reference wavelength of 650 nm was determined with a multifunctional microplate reader (Tecan Infinite M200).

Conflict of Interest: The authors declare no competing financial interest.

Acknowledgment. This work was supported by the National Basic Research Program of China (973 Program, 2013CB932701), the 100-Talent Program of the Chinese Academy of Sciences, National Natural Science Foundation of China (21374026, 21304023, and 51303036), and Beijing Natural Science Foundation (2132053). L.-L.L. thanks the China Postdoctoral Science Foundation (2013M540902) for financial support.

Supporting Information Available: TEM images of SGNPs@RBC and SLO-absorbing SGNPs@RBC, standard curve of Van measured by HPLC, representative time-dependent Van release curves of Van⊂SGNPs@RBC, Van⊂SGNPs, and photographs of the antihemolysis of the SGNPs@RBC to SLO. This material is available free of charge *via* the Internet at http://pubs.acs.org.

REFERENCES AND NOTES

1. Levin, B. R.; Antia, R. Why We Don't Get Sick: The Within-Host Population Dynamics of Bacterial Infections. *Science* **2001**, *292*, 1112–1115.
2. Davies, J.; Davies, D. Origins and Evolution of Antibiotic Resistance. *Microbiol. Mol. Biol. Rev.* **2010**, *74*, 417–433.
3. Levy, S. B.; Marshall, B. Antibacterial Resistance Worldwide: Causes, Challenges and Responses. *Nat. Med.* **2004**, *10*, S122–S129.
4. Smith, A. W. Biofilms and Antibiotic Therapy: Is There a Role for Combating Bacterial Resistance by the Use of Novel Drug Delivery Systems? *Adv. Drug Delivery Rev.* **2005**, *57*, 1539–1550.
5. Tarpley, R. J. Antibiotics: Discontinue Low-Dose Use. *Science* **2014**, *343*, 136–137.
6. Sun, T.; Qing, G. Biomimetic Smart Interface Materials for Biological Applications. *Adv. Mater.* **2011**, *23*, H57–H77.
7. Agarwal, A.; Guthrie, K. M.; Czuprynski, C. J.; Schurr, M. J.; McAnulty, J. F.; Murphy, C. J.; Abbott, N. L. Polymeric Multilayers That Contain Silver Nanoparticles Can Be Stamped onto Biological Tissues to Provide Antibacterial Activity. *Adv. Funct. Mater.* **2011**, *21*, 1863–1873.
8. Lee, J. S.; Murphy, W. L. Functionalizing Calcium Phosphate Biomaterials with Antibacterial Silver Particles. *Adv. Mater.* **2013**, *25*, 1173–1179.
9. Zhao, Y.; Tian, Y.; Cui, Y.; Liu, W.; Ma, W.; Jiang, X. Small Molecule-Capped Gold Nanoparticles as Potent Antibacterial Agents That Target Gram-Negative Bacteria. *J. Am. Chem. Soc.* **2010**, *132*, 12349–12356.
10. Lv, M.; Su, S.; He, Y.; Huang, Q.; Hu, W.; Li, D.; Fan, C.; Lee, S.-T. Long-Term Antimicrobial Effect of Silicon Nanowires Decorated with Silver Nanoparticles. *Adv. Mater.* **2010**, *22*, 5463–5467.
11. Zhang, D.; Zhao, Y.-X.; Gao, Y.-J.; Gao, F.-P.; Fan, Y.-S.; Li, X.-J.; Duan, Z.-Y.; Wang, H. Anti-Bacterial and *in Vivo* Tumor Treatment by Reactive Oxygen Species Generated by Magnetic Nanoparticles. *J. Mater. Chem. B* **2013**, *1*, 5100–5107.
12. Ocsoy, I.; Paret, M. L.; Ocsoy, M. A.; Kunwar, S.; Chen, T.; You, M.; Tan, W. Nanotechnology in Plant Disease Management: DNA-Directed Silver Nanoparticles on Graphene Oxide as an Antibacterial against Xanthomonas Perforans. *ACS Nano* **2013**, *7*, 8972–8980.
13. Qi, G.; Li, L.; Yu, F.; Wang, H. Vancomycin-Modified Mesoporous Silica Nanoparticles for Selective Recognition and Killing of Pathogenic Gram-Positive Bacteria over Macrophage-Like Cells. *ACS Appl. Mater. Interfaces* **2013**, *5*, 10874–10881.
14. Li, L.-l.; Wang, H. Enzyme-Coated Mesoporous Silica Nanoparticles as Efficient Antibacterial Agents in Vivo. *Adv. Healthcare Mater.* **2013**, *2*, 1351–1360.
15. Wu, M.-C.; Deokar, A. R.; Liao, J.-H.; Shih, P.-Y.; Ling, Y.-C. Graphene-Based Photothermal Agent for Rapid and Effective Killing of Bacteria. *ACS Nano* **2013**, *7*, 1281–1290.
16. Li, Y.; Zhang, W.; Niu, J.; Chen, Y. Mechanism of Photogenerated Reactive Oxygen Species and Correlation with the Antibacterial Properties of Engineered Metal-Oxide Nanoparticles. *ACS Nano* **2012**, *6*, 5164–5173.
17. Some, S.; Ho, S. M.; Dua, P.; Hwang, E.; Shin, Y. H.; Yoo, H.; Kang, J. S.; Lee, D. K.; Lee, H. Dual Functions of Highly Potent Graphene Derivative-Poly-L-Lysine Composites to Inhibit Bacteria and Support Human Cells. *ACS Nano* **2012**, *6*, 7151–7161.
18. Salick, D. A.; Pochan, D. J.; Schneider, J. P. Design of an Injectable β-Hairpin Peptide Hydrogel That Kills Methicillin-Resistant Staphylococcus aureus. *Adv. Mater.* **2009**, *21*, 4120–4123.
19. Liu, L.; Xu, K.; Wang, H.; Jeremy Tan, P. K.; Fan, W.; Venkatraman, S. S.; Li, L.; Yang, Y.-Y. Self-Assembled Cationic Peptide Nanoparticles as An Efficient Antimicrobial Agent. *Nat. Nanotechnol.* **2009**, *4*, 457–463.
20. Adhikari, M. D.; Goswami, S.; Panda, B. R.; Chattopadhyay, A.; Ramesh, A. Membrane-Directed High Bactericidal Activity of (Gold Nanoparticle)−Polythiophene Composite for Niche Applications against Pathogenic Bacteria. *Adv. Healthcare Mater.* **2013**, *2*, 599–606.
21. Lee, H.; Lee, Y.; Statz, A. R.; Rho, J.; Park, T. G.; Messersmith, P. B. Substrate-Independent Layer-by-Layer Assembly by Using Mussel-Adhesive-Inspired Polymers. *Adv. Mater.* **2008**, *20*, 1619–1623.
22. Li, P.; Zhou, C.; Rayatpisheh, S.; Ye, K.; Poon, Y. F.; Hammond, P. T.; Duan, H.; Chan-Park, M. B. Cationic Peptidopolysaccharides Show Excellent Broad-Spectrum Antimicrobial Activities and High Selectivity. *Adv. Mater.* **2012**, *24*, 4130–4137.
23. Zhou, Y.; Huang, W.; Liu, J.; Zhu, X.; Yan, D. Self-Assembly of Hyperbranched Polymers and Its Biomedical Applications. *Adv. Mater.* **2010**, *22*, 4567–4590.

24. Ng, V. W. L.; Ke, X.; Lee, A. L. Z.; Hedrick, J. L.; Yang, Y. Y. Synergistic Co-delivery of Membrane-Disrupting Polymers with Commercial Antibiotics against Highly Opportunistic Bacteria. *Adv. Mater.* **2013**, *25*, 6730–6736.
25. Sémiramoth, N.; Meo, C. D.; Zouhiri, F.; Saïd-Hassane, F.; Valetti, S.; Gorges, R.; Nicolas, V.; Poupaert, J. H.; Chollet-Martin, S.; Desmaële, D.; Gref, R.; Couvreur, P. Self-Assembled Squalenoylated Penicillin Bioconjugates: An Original Approach for the Treatment of Intracellular Infections. *ACS Nano* **2012**, *6*, 3820–3831.
26. Xiong, M.-H.; Li, Y.-J.; Bao, Y.; Yang, X.-Z.; Hu, B.; Wang, J. Bacteria-Responsive Multifunctional Nanogel for Targeted Antibiotic Delivery. *Adv. Mater.* **2012**, 6175–6180.
27. Wang, G.; Pahari, P.; Kharel, M. K.; Chen, J.; Zhu, H.; Van Lanen, S. G.; Rohr, J. Cooperation of Two Bifunctional Enzymes in the Biosynthesis and Attachment of Deoxysugars of the Antitumor Antibiotic Mithramycin. *Angew. Chem., Int. Ed.* **2012**, *51*, 10638–10642.
28. Campoccia, D.; Montanaro, L.; Speziale, P.; Arciola, C. R. Antibiotic-Loaded Biomaterials and the Risks for the Spread of Antibiotic Resistance Following Their Prophylactic and Therapeutic Clinical Use. *Biomaterials* **2010**, *31*, 6363–6377.
29. Zhang, S.; Chu, Z.; Yin, C.; Zhang, C.; Lin, G.; Li, Q. Controllable Drug Release and Simultaneously Carrier Decomposition of SiO_2-Drug Composite Nanoparticles. *J. Am. Chem. Soc.* **2013**, *135*, 5709–5716.
30. Dantas, G.; Sommer, M. O. A.; Oluwasegun, R. D.; Church, G. M. Bacteria Subsisting on Antibiotics. *Science* **2008**, *320*, 100–103.
31. Proctor, R. A.; Peters, G. Small Colony Variants in Staphylococcal Infections: Diagnostic and Therapeutic Implications. *Clin. Infect. Dis.* **1998**, *27*, 419–422.
32. Garzoni, C.; Kelley, W. L. Return of The Trojan Horse: Intracellular Phenotype Switching and Immune Evasion by *Staphylococcus aureus*. *EMBO Mol. Med.* **2011**, *3*, 115–117.
33. Radovic-Moreno, A. F.; Lu, T. K.; Puscasu, V. A.; Yoon, C. J.; Langer, R.; Farokhzad, O. C. Surface Charge-Switching Polymeric Nanoparticles for Bacterial Cell Wall-Targeted Delivery of Antibiotics. *ACS Nano* **2012**, *6*, 4279–4287.
34. Tanihara, M.; Suzuki, Y.; Nishimura, Y.; Suzuki, K.; Kakimaru, Y.; Fukunishi, Y. A Novel Microbial Infection-Responsive Drug Release System. *J. Pharm. Sci.* **1999**, *88*, 510–514.
35. Hubbell, J. A.; Chilkoti, A. Nanomaterials for Drug Delivery. *Science* **2012**, *337*, 303–305.
36. Bourzac, K. Nanotechnology: Carrying Drugs. *Nature* **2012**, *491*, S58–S60.
37. Hu, C.-M. J.; Fang, R. H.; Copp, J.; Luk, B. T.; Zhang, L. A Biomimetic Nanosponge that Absorbs Pore-Forming Toxins. *Nat. Nanotechnol.* **2013**, *8*, 336–340.
38. Hu, C. M.; Zhang, L.; Aryal, S.; Cheung, C.; Fang, R. H. Erythrocyte Membrane-Camouflaged Polymeric Nanoparticles as a Biomimetic Delivery Platform. *Proc. Natl. Acad. Sci. U.S.A.* **2011**, *108*, 10980–10985.
39. Haag, R. Supramolecular Drug-Delivery Systems Based on Polymeric Core–Shell Architectures. *Angew. Chem., Int. Ed.* **2004**, *43*, 278–282.
40. Chen, G.; Jiang, M. Cyclodextrin-Based Inclusion Complexation Bridging Supramolecular Chemistry and Macromolecular Self-Assembly. *Chem. Soc. Rev.* **2011**, *40*, 2254–2266.
41. Yan, X.; Wang, F.; Zheng, B.; Huang, F. Stimuli-Responsive Supramolecular Polymeric Materials. *Chem. Soc. Rev.* **2012**, *41*, 6042–6065.
42. Zhang, X.; Wang, C. Supramolecular Amphiphiles. *Chem. Soc. Rev.* **2011**, *40*, 94–101.
43. Wang, L.; Li, L. L.; Fan, Y. S.; Wang, H. Host-Guest Supramolecular Nanosystems for Cancer Diagnostics and Therapeutics. *Adv. Mater.* **2013**, *25*, 3888–98.
44. Kholmanov, I. N.; Stoller, M. D.; Edgeworth, J.; Lee, W. H.; Li, H.; Lee, J.; Barnhart, C.; Potts, J. R.; Piner, R.; Akinwande, D.; Barrick, J. E.; Ruoff, R. S. Nanostructured Hybrid Transparent Conductive Films with Antibacterial Properties. *ACS Nano* **2012**, *6*, 5157–5163.
45. Fukushima, K.; Tan, J. P. K.; Korevaar, P. A.; Yang, Y. Y.; Pitera, J.; Nelson, A.; Maune, H.; Coady, D. J.; Frommer, J. E.; Engler, A. C.; Huang, Y.; Xu, K.; Ji, Z.; Qiao, Y.; Fan, W.; Li, L.; Wiradharma, N.; Meijer, E. W.; Hedrick, J. L. Broad-Spectrum Antimicrobial Supramolecular Assemblies with Distinctive Size and Shape. *ACS Nano* **2012**, *6*, 9191–9199.
46. Xu, X.; Yuan, H.; Chang, J.; He, B.; Gu, Z. Cooperative Hierarchical Self-Assembly of Peptide Dendrimers and Linear Polypeptides into Nanoarchitectures Mimicking Viral Capsids. *Angew. Chem., Int. Ed.* **2012**, *51*, 3130–3133.
47. Chakrabarty, R.; Mukherjee, P. S.; Stang, P. J. Supramolecular Coordination: Self-Assembly of Finite Two- and Three-Dimensional Ensembles. *Chem. Rev.* **2011**, *111*, 6810–6918.
48. Jin, H.; Huang, W.; Zhu, X.; Zhou, Y.; Yan, D. Biocompatible or Biodegradable Hyperbranched Polymers: From Self-Assembly to Cytomimetic Applications. *Chem. Soc. Rev.* **2012**, *41*, 5986–5997.
49. Uhlenheuer, D. A.; Petkau, K.; Brunsveld, L. Combining Supramolecular Chemistry with Biology. *Chem. Soc. Rev.* **2010**, *39*, 2817–2826.
50. Wang, H.; Wang, S.; Su, H.; Chen, K.-J.; Armijo, A. L.; Lin, W.-Y.; Wang, Y.; Sun, J.; Kamei, K.-i.; Czernin, J.; Radu, C. G.; Tseng, H.-R. A Supramolecular Approach for Preparation of Size-Controlled Nanoparticles. *Angew. Chem., Int. Ed.* **2009**, *48*, 4344–4348.
51. Ethirajan, A.; Schoeller, K.; Musyanovych, A.; Ziener, U.; Landfester, K. Synthesis and Optimization of Gelatin Nanoparticles Using the Miniemulsion Process. *Biomacromolecules* **2008**, *9*, 2383–2389.
52. Naidu, B. V. K.; Paulson, A. T. A New Method for the Preparation of Gelatin Nanoparticles: Encapsulation and Drug Release Characteristics. *J. Appl. Polym. Sci.* **2011**, *121*, 3495–3500.
53. Xu, J.-H.; Gao, F.-P.; Liu, X.-F.; Zeng, Q.; Guo, S.-S.; Tang, Z.-Y.; Zhao, X.-Z.; Wang, H. Supramolecular Gelatin Nanoparticles as Matrix Metalloproteinase Responsive Cancer Cell Imaging Probes. *Chem. Commun.* **2013**, *49*, 4462–4464.
54. Forsyth, P. A.; Wong, H.; Laing, T. D.; Rewcastle, N. B.; Morris, D. G.; Muzik, H.; Leco, K. J.; Johnston, R. N.; Brasher, P. M.; Sutherland, G.; Edwards, D. R. Gelatinase-A (MMP-2), Gelatinase-B (MMP-9) and Membrane Type Matrix Metalloproteinase-1 (MT1-MMP) Are Involved in Different Aspects of the Pathophysiology of Malignant Gliomas. *Br. J. Cancer* **1999**, *79*, 1828–1835.
55. Toth, M.; Sohail, A.; Fridman, R. Assessment of Gelatinases (MMP-2 and MMP-9) by Gelatin Zymography. In *Metastasis Research Protocols*; Dwek, M.; Brooks, S. A.; Schumacher, U., Eds.; Humana Press, 2012; Vol. 878, pp 121–135.
56. Azzopardi, E. A.; Ferguson, E. L.; Thomas, D. W. The Enhanced Permeability Retention Effect: A New Paradigm for Drug Targeting in Infection. *J. Antimicrob. Chemother.* **2013**, *68*, 257–274.
57. Xu, J.-H.; Gao, F.-P.; Li, L.-L.; Ma, H. L.; Fan, Y.-S.; Liu, W.; Guo, S.-S.; Zhao, X.-Z.; Wang, H. Gelatin–Mesoporous Silica Nanoparticles as Matrix Metalloproteinases-Degradable Drug Delivery Systems *in Vivo*. *Microporous Mesoporous Mater.* **2013**, *182*, 165–172.
58. Hochmuth, R.; Evans, C.; Wiles, H.; McCown, J. Mechanical Measurement of Red Cell Membrane Thickness. *Science* **1983**, *220*, 101–102.
59. Tilley, S. J.; Saibil, H. R. The Mechanism of Pore Formation by Bacterial Toxins. *Curr. Opin. Struct. Biol.* **2006**, *16*, 230–236.
60. Peterson, J. W. In *Bacterial Pathogenesis*; Baron, S., Ed.; Medical Microbiology: Galveston, TX, 1996; Vol. 7.